Journal of Power Sources 187 (2009) 32–38

Contents lists available at ScienceDirect

Journal of Power Sources

journal homepage: www.elsevier.com/locate/jpowsour

Potential dependence of sulfur dioxide poisoning and oxidation at the cathode of proton exchange membrane fuel cells

Jie Fu[a,b], Ming Hou[a,*], Chao Du[a,b], Zhigang Shao[a], Baolian Yi[a]

[a] Fuel Cell System and Engineering Research Group, Dalian Institute of Chemical Physics, Chinese Academy of Science, 457 Zhongshan Road, Dalian 116023, PR China
[b] Graduate School of the Chinese Academy of Sciences, Beijing 100039, PR China

ARTICLE INFO

Article history:
Received 14 October 2008
Accepted 20 October 2008
Available online 6 November 2008

Keywords:
Proton exchange membrane fuel cell
Sulfur dioxide
Potential dependence
Poisoning
Oxidation

ABSTRACT

Cyclic voltammetry (CV) and electrochemical impedance spectroscopy (EIS) were employed to investigate changes in the cathode after the introduction of SO_2. The decay in performance of the proton exchange membrane fuel cell (PEMFC) was ascribed to the increasing of the charge transfer resistance (R_{ct}) caused by the loss of the electrochemical surface area (ECA). The results show that the oxidation and adsorption behaviors of SO_2 depended closely on the potential. Adsorbed sulfur began to be oxidized over 0.9 V and could be oxidized completely with CV maximum potentials up to 1.05 V or higher. At about 0.65 V, the adsorbed SO_2 was probably in a molecular state, which could be reduced in the range of 0.65–0.05 V. Some SO_2 molecules occupied initially two Pt sites through S and O. One of the two sites could be released after the reduction. The increasing of ECA due to reduction could lessen the impact of SO_2 on the PEMFC performance at voltages below 0.65 V.

1. Introduction

Proton exchange membrane fuel cells (PEMFCs) have been used in vehicles due to their relatively low operating temperatures and start-up as well as transient-response in a short time. For ambient air compressed directly into the cathode as the oxidant, the performance of the PEMFC depends significantly on the quality of the ambient air. It has been proved that the impurities in the air impacted negatively on the performance and the durability of the fuel cells. Among these impurities, sulfur-containing compounds in the air, especially sulfur dioxide, are the most deleterious to PEMFCs [1].

Poisoning of the cathode catalyst resulting from SO_2 is irreversible [2]. The adsorption of impurities on the catalyst surface can cause loss in Pt surface sites which are necessary for the oxygen reduction reaction (ORR), or in other words, a decrease in the active area [3–5]. Motadi et al. [6] demonstrated that the cell performance decreased by 53% after running with 2.5 ppm SO_2/air for 45 h and it could not be recovered by running again with pure air for 20 h. Uribe et al. [7] investigated the performances of fuel cells the cathodes of which were exposed to air containing 1 and 5 ppm SO_2, respectively. Performance degradations were found for both of the impurity levels, and the effect with the higher impurity concentration was faster and more acute, as could be expected. Furthermore, even 250 ppb SO_2 could cause a distinct decay of the cell performance [2].

On account of the severe impact of SO_2, several methods have been used to recover the poisoned cells and improve the durability of the PEMFCs. Cycle voltammetry (CV) has been regarded as an alternative method. In situ voltammetric polarization (CV up to 1.4 V vs. DHE) could result in a complete reactivation of the cathode catalyst [4–6]. This reactivation could not take place during normal cell operation [2], but open circuit voltage (OCV) application on the sulfur-poisoned electrodes [7] or an *I–V* measurement of the fuel cell [4] indicated a partial recovery. All these facts showed that sulfur species adsorbed on the platinum surface could be oxidized and desorbed at high potentials [4–9].

The adsorption behavior of SO_2 on the surface of platinum is extremely complicated and the surface states show high potential dependence [9–17]. The nature of the sulfur species adsorbed on platinum in solutions has been studied. It was found that at 0.05 V, the sulfur was in a zero-valence state [9]. When SO_2 was introduced at 0.2 V or below, colloidal sulfur appeared in the solution [11]. Oxidation and reduction of the SO_2 occurred on polycrystalline Pt electrodes at potentials higher and lower than 0.65 V, respectively, with an uncharged product of SO_2 adsorption at 0.65 V [12]. Sulfur compounds adsorbed on Pt tended to be oxidized to SO_4^{2-} at 0.9 V or higher potentials in the fuel cells [4]. Two distinct oxidation peaks, one at 0.97 V, corresponding to weakly bound sulfur, and the other at 1.20 V, corresponding to strongly bound sulfur, were observed at 80 °C [13]. At potentials higher than 1.2 V, oxygen

* Corresponding author. Tel.: +86 411 84379051; fax: +86 411 84379185.
E-mail address: houming@dicp.ac.cn (M. Hou).

0378-7753/$ – see front matter © 2008 Elsevier B.V. All rights reserved.
doi:10.1016/j.jpowsour.2008.10.103

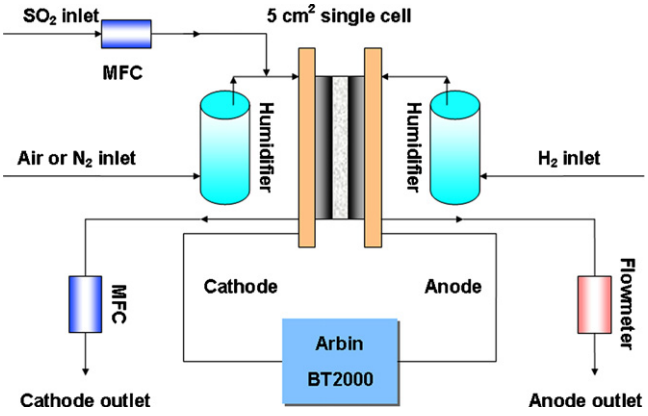

Fig. 1. Sketch of PEMFC single cell assessing system.

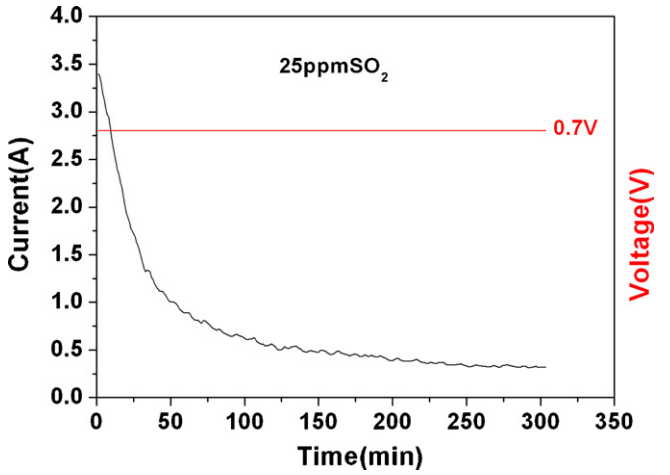

Fig. 2. Effect of 25 ppm SO_2 in the air on the PEMFC performance. T_{cell} = 70 °C, humidification temperatures of the anode and the cathode: 70 °C.

adsorption began to prevail and block platinum sites so that the oxidation of SO_2 was inhibited [15].

In summary, most of the studies mentioned above were conducted in solutions where the circumstances were different from that of a PEMFC. In this paper, methods such as CV and electrochemical impedance spectroscopy (EIS) were used to investigate the effect of the potential on SO_2 poisoning and oxidation during the operation of the PEMFCs and analyze the impact of adsorbed sulfur species on electrodes.

2. Experimental

All experiments were performed with a single cell, the active area of which was 5 cm^2. The membrane electrode assembly (MEA), which was comprised of a Nafion® 212 membrane (Dupont) and two electrodes, was prepared by warming-up for 60 s and then hot pressing at 140 °C and 10 MPa for 60 s. Each electrode was supported by Toray carbon paper (Japan). Both the cathode and the anode had a Pt loading of 0.4 mg cm^{-2}. Stainless steel end plates and flexible graphite flow fields were used to assemble single cells.

A sketch of the PEMFC single cell assessing system is shown in Fig. 1. The gases used were high purity H_2, neat air, high purity N_2 and standardized SO_2 balanced with air. SO_2 was mixed into moist air or N_2 which had been humidified in order to avoid being adsorbed by water. The flow rate of the standardized SO_2 was controlled by a mass flow controller (MFC). Comparing to humidified air, the flux of SO_2 was much smaller. So the humidity of the mixed gases at the cathode inlet was virtually not affected. Another MFC was also used to control the total flux at the cathode outlet. The actual concentration of the SO_2 fed into the cathode could be calculated with the given flow rates of both the standardized SO_2 and air. The flux of hydrogen was measured by a flowmeter.

During the experiments, the cell temperature and the humidification temperature were both 70 °C. The flux of pure hydrogen was 30 sccm (standard cubic centimeter per minute) and that of the reacting gas (air or SO_2/air) on the cathode side was 500 sccm. The pressures of the reacting gases were 0.1 MPa(g) on both sides. The single cell was tested with constant-voltage discharge by Arbin BT2000 (America, Arbin Instruments) and the current–time (C–t) curves were also automatically recorded by it. Thus the decay of the current during the continual injection of SO_2/air to the cathode could be investigated. All the CV measurements were performed by a PARSTAT 2273 electrochemical station (America, EG&G Instruments Corp.). The cathode was acting as the working electrode where high purity nitrogen was flowing with the rate of 200 sccm. Meanwhile, pure hydrogen was flowing on the anode side with the rate of 30 sccm to act as the reference and counter electrode. The applied potential range was chosen according to the purpose, and the scanning rate was 50 mV s^{-1}. EIS measurements were also performed by the PARSTAT 2273. The impedance spectra were recorded by sweeping various frequencies in the range of 10 kHz to 100 mHz. During all the EIS measurements, the potential was fixed at 0.7 V to ensure the same polarization.

3. Results and discussion

3.1. The influence of SO_2 on the cathode of PEMFC

3.1.1. Effect of SO_2 on R_{ct}

The effect of 25 ppm SO_2 in air on the PEMFC performance is shown in Fig. 2. After activation, the single cell was operated potentiostatically at 0.7 V till the current became stable, and then 25 ppm SO_2 was introduced into the cathode. It can be observed in Fig. 2 that the current decreases rapidly at the initial tens of minutes, and then tends to become a platform shape. This curve is similar to the one obtained by operating the cell galvanostatically [1,2,5,7]. The decay in current is ascribed to the adsorption of sulfur dioxide on the Pt active sites that are necessary for the ORR.

The cyclic voltammetry spectra of the cathode were measured in different periods when the cathode was exposed to 25 ppm SO_2 at 0.7 V (Fig. 3). The scanning range was limited from 0.05 to 0.5 V in order to avoid oxidation of the adsorbed sulfur at higher potentials. From Fig. 3, we can see that the electrochemical surface area (ECA) corresponding to the H-desorption peak area is getting smaller during the poisoning process.

Meanwhile, impedance spectra were also obtained during the running of the poisoning process. Nyquist plots are shown in Fig. 4. Each of them has a similar pattern: an inductive line at the high frequency range, and a depressed capacitive semicircle at the intermediate and low frequency range. Fig. 4 reveals that arcs relating to charge transfer increase with the continuous input of SO_2.

An equivalent circuit (EC) of the single cell, as shown in Fig. 5, is employed to describe quantitatively the change of the impedance. The inductance (L) corresponding to the inductive lines in the Nyquist plots derives from the metal wires and the stainless steel end plates. The inductive lines intersect the real axis at R_{hf}, reflecting the total ohmic resistance of the cell. The capacitance of the double-layer is distinctive from the simple capacitance, and can be represented by a constant phase angle element (CPE). The charge transfer resistance (R_{ct}) at the electrode–membrane interface is

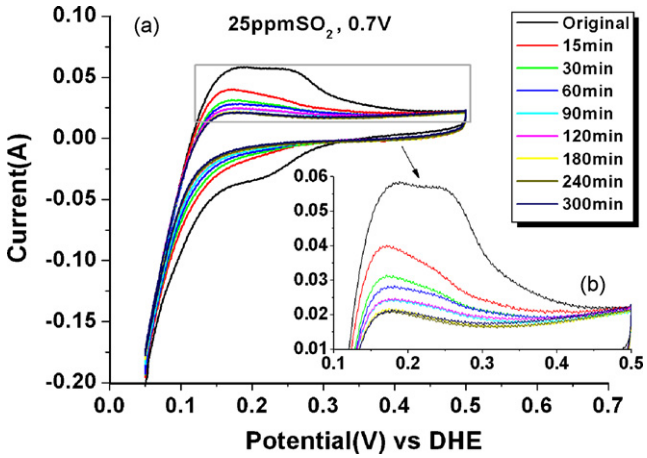

Fig. 3. (a) Cyclic voltammetry spectra obtained in different periods during the cathode exposure to 25 ppm SO_2 at 0.7 V and (b) enlarged part of the H-desorption peak in cyclic voltammetry spectra. T_{cell} = 70 °C, humidification temperatures of the anode and the cathode: 70 °C.

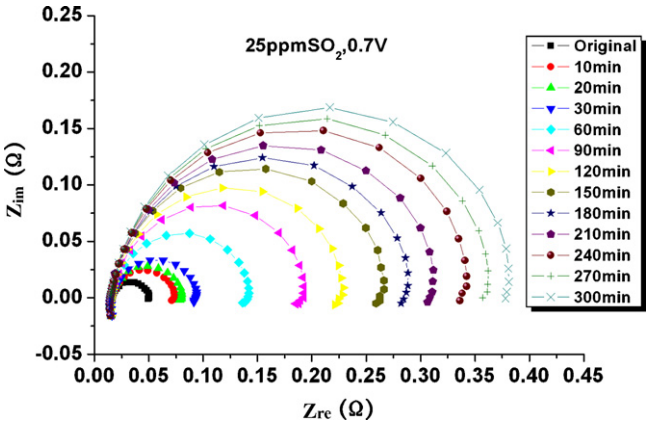

Fig. 4. Impedance spectra obtained in different periods during the cathode exposure to 25 ppm SO_2 at 0.7 V. T_{cell} = 70 °C, humidification temperatures of the anode and the cathode: 70 °C.

associated with the presence of mixed conduction (protonic and electronic) at this interface.

Due to the fact that anode polarization is negligible against cathode polarization during the fuel cell operation, the cathode impedance can be replaced by the total impedance [18]. The calculated parameters of the EC are listed in Table 1.

From Table 1, it can be seen that L, R_{hf}, CPE and n (excursion of the arc to semicircle) were almost invariable on the whole, with only the R_{ct} ascended as the cathode was poisoned. This result implies that the adsorption of the active oxygen atoms on the Pt surface was blocked. The H-desorption peak area of each cycle in Fig. 3 was integrated to get the values of ECA in different periods. The relationship between the ECA and R_{ct} is plotted in Fig. 6, which shows that the descending of the ECA is accompanied with the ascending of the R_{ct}. When the cathode was poisoned, the constant voltage of the cell implied that the driving force for charge transfer was invariable. However, the Pt active sites for the ORR had decreased with the input of the SO_2, so the charge transfer resistance went up. Consequently, less current could be discharged.

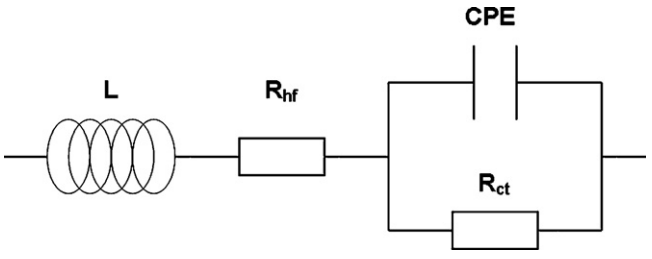

Fig. 5. Equivalent circuit of the single cell.

Table 1
Calculated values from equivalent circuit.

Time (min)	$L \times 10^7$ (H)	R_{hf} (Ω)	CPE (S s^{-n})	n	R_{ct} (Ω)
0	2.49	15.26	0.1544	0.8432	35.35
10	2.47	16.14	0.1098	0.8842	57.71
20	2.48	14.97	0.1073	0.8906	65.66
30	2.46	16.07	0.1033	0.8958	78.02
60	2.45	15.29	0.0885	0.9224	126.0
90	2.45	15.76	0.0885	0.9236	178.0
120	2.46	15.2	0.0922	0.9204	214.5
150	2.46	14.83	0.0941	0.9194	253.9
180	2.48	14.41	0.1014	0.9094	278.2
210	2.47	14.57	0.1002	0.9122	302.1
240	2.48	14.40	0.1036	0.9088	334.4
270	2.48	14.28	0.1023	0.9103	355.1
300	2.47	14.48	0.1032	0.9091	375.3

3.1.2. *Effect of sulfur coverage on ECA*

Fig. 7 shows the cyclic voltammetry spectra of the cathode before and after being poisoned at 0.7 V by 25 ppm SO_2 for 5 h. The difference in H-desorption peak areas reflects the Pt active sites covered by the adsorbed sulfur, and the difference in O-oxidation peak areas corresponds to the charges produced by the oxidation of the adsorbed sulfur. It also can be seen in Fig. 7 that the O-oxidation peaks began to deviate at about 0.925 V. It indicates that oxidation of the adsorbed sulfur started approximately at this potential. The reaction rate increased as the adsorbed sulfur was oxidatively desorbed and a greater number of the Pt sites became available. Meanwhile, two separate processes, i.e. oxidation of SO_2 and adsorption of oxygen, competed for the free sites. However, the formation of surface oxides began to predominate beyond 1.20 V. Accordingly, the oxidation of SO_2 was restrained.

It has been reported that sulfur is in a zero-valence state (Pt–S) at 0.05 V [3]. On the other hand, at potentials higher than 0.9 V, the sulfur adsorbed on Pt is easily electro-oxidized to the sulfate (SO_4^{2-}) due to the following reaction [4]:

$$Pt\text{–}S + 4H_2O \rightarrow SO_4^{2-} + 8H^+ + 6e^- + Pt \quad (1)$$

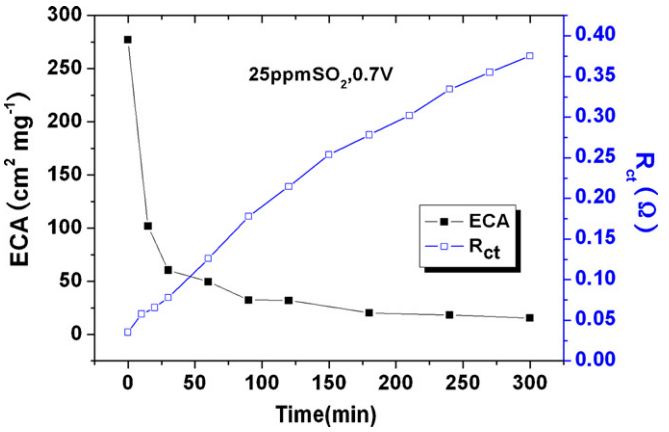

Fig. 6. Correlation between ECA and R_{ct} in different periods during the cathode exposure to 25 ppm SO_2 at 0.7 V. T_{cell} = 70 °C, humidification temperatures of the anode and the cathode: 70 °C.

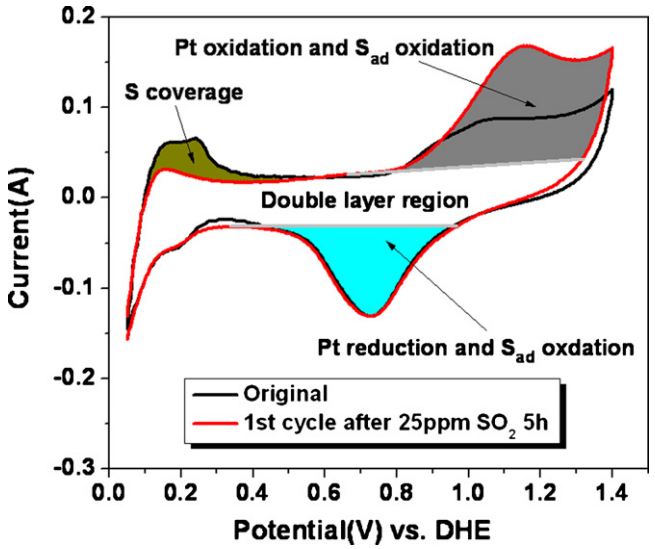

Fig. 7. Comparison of cyclic voltammetry spectra of the cathode before and after being poisoned by 25 ppm SO_2 for 5 h at 0.7 V. T_{cell} = 70 °C, humidification temperatures of the anode and the cathode: 70 °C.

Therefore, when the adsorbed sulfur was performed CV scan from 0.05 to 1.4 V, a 6-electron transfer process occurred. As shown in Fig. 7, the peak area of O-oxidation is corresponding to the charge sum of the Pt oxidation (Q_{ox}^{Pt}) and the adsorbed sulfur oxidation (Q_{ox}^{S1}) in this region, that is

$$Q_{ox} = Q_{ox}^{Pt} + Q_{ox}^{S1} \tag{2}$$

And the peak area of O-reduction is corresponding to the charge difference of the Pt reduction (Q_{re}^{Pt}) and the adsorbed sulfur oxidation (Q_{ox}^{S2}) in the region, that is

$$Q_{re} = Q_{re}^{Pt} - Q_{ox}^{S2} \tag{3}$$

Q_{ox}^{Pt} and Q_{re}^{Pt} could counteract with each other, so the difference between the two peak areas represents the total sulfur oxidation charges (Q_{ox}^{S}) in this cycle, which can be expressed as

$$Q_{ox}^{S} = Q_{ox} - Q_{re} = Q_{ox}^{S1} + Q_{ox}^{S2} \tag{4}$$

Thus, the quantities of the sulfur oxidized and desorbed from the Pt surface in each cycle could be obtained. Accordingly, the relationship between the surface sulfur coverage and the ECA could be clarified.

The CV was chosen to investigate the impact of the adsorbed SO_2 on the state of the Pt surface. The cell temperature and the humidification temperature were both 70 °C. 25 ppm SO_2 in air was introduced into the cathode for 5 h when the cell voltage was fixed at 0.7 V. After being poisoned, the cathode was exposed to high purity N_2 and performed CV. All minima of the potentials in each cycle were 0.05 V and the maxima increased from 0.75 to 1.4 V with steps of 0.05 V, respectively. The CV in each range was performed twice. All curves are exhibited in Fig. 8. A gradual recovery of the ECA can be observed with the increasing of the maximum potentials. By using Eqs. (5)–(7), we can get θ_S^i and θ_H^i, representing the coverages of Pt active sites occupied by S and H after cycle *i*.

$$Q_{ox}^{S} = \frac{A_{ox}^{O} - A_{re}^{O}}{u} \tag{5}$$

$$\theta_S^i = \frac{\sum Q_{ox}^{S} - \sum_{1,i-1} Q_{ox}^{S}}{6Q_H^*} \tag{6}$$

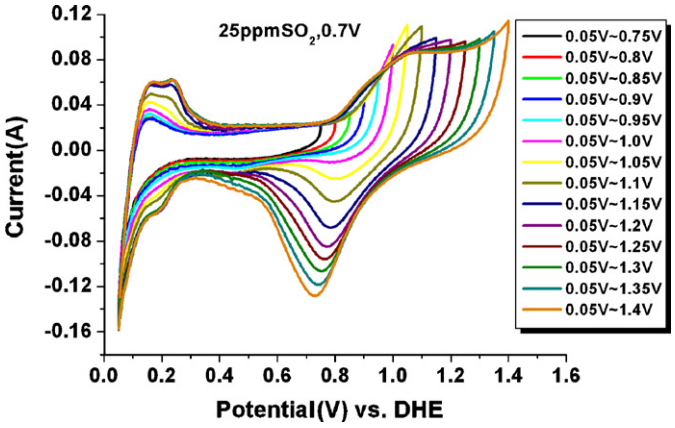

Fig. 8. Cyclic voltammetry recovery spectra with different scan ranges after the cathode being exposed to 25 ppm SO_2 for 5 h at 0.7 V. T_{cell} = 70 °C, humidification temperatures of the anode and the cathode: 70 °C.

$$\theta_H^i = \frac{Q_H^i}{Q_H^*} \tag{7}$$

where Q_{ox}^{S} is the charge of sulfur oxidation, A_{ox}^{O} and A_{re}^{O} are the integral areas of the O-oxidation peak and O-reduction peak, respectively, *u* is the potential scanning rate, Q_H^i and Q_H^* are respectively the charges corresponding to H-desorption from the Pt active sites in cycle *i* and in the original cycle before poisoning.

Calculated values of θ_S^i and θ_H^i in the second cycle of each range are plotted in Fig. 9. It revealed that the θ_S decreased gradually with the increasing of the maximum potential over 0.9 V. Meanwhile, θ_H was getting close to 100%. Moreover, $\theta_S + \theta_H$ was approaching 100% all the time. This result indicates that the assumption of the adsorbed sulfur being in a zero-valence state and combining with one Pt atom at 0.05 V is reliable, and the loss of the ECA can be mostly ascribed to the sulfur coverage.

3.2. Potential dependence of sulfur oxidation

3.2.1. The influence of the maximum potentials in CV

Although oxidation and desorption of sulfur can be determined via CV, the recovery effect depends on the maximum potentials of the cycles. 25 ppm SO_2 in the air feed was introduced into the cath-

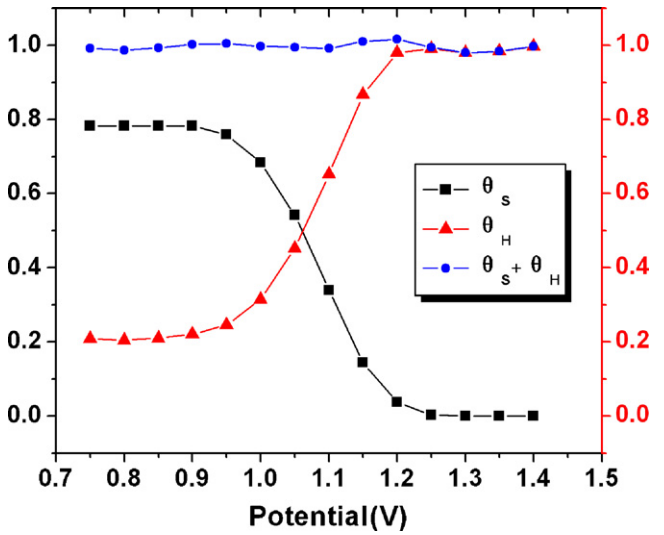

Fig. 9. Comparison of θ_S, θ_H and $\theta_S + \theta_H$.

Table 2
Integration results of ECA recovery percent with different CV maximum potentials.

CV maximum	Recovery percent
0.75 V	23.35
0.8 V	23.35
0.85 V	23.35
0.9 V	23.35
0.95 V	46.17
1 V	80.31
1.05 V	98.08
1.1 V	98.26
1.15 V	98.96
1.2 V	98.78
1.25 V	98.61
1.3 V	98.43
1.35 V	98.31
1.4 V	98.26

ode for 5 h at 0.7 V. The cell temperature and the humidification temperature were both 70 °C. After the poisoning test, CV scans with various ranges, as shown in Section 3.1.2, were performed. The maximum potentials did not change until the ECA of the catalyst became stable. After the CV scans, the H-desorption peak area of each cycle was integrated separately and compared with that obtained before poisoning (100%). The result of integration is shown in Table 2.

From Table 2, it can be seen that the ECA did not recover until the CV maximum reached 0.95 V. A recovery of only 46.17% could be attained even after 25 cycles, with an upper limit of 0.95 V. The result implies that only partial recovery could be obtained in this range, and further release of the remaining sulfur-covered Pt sites needed higher potentials. Analogously, when the maximum potential was 1.0 V, only 80.31% of the Pt surface sites were active. On the other hand, when the maximum potential had reached 1.05 V, nearly a total ECA recovery could be attained. The difference between the ECA after high potential recovery and that before poisoning was caused by dissolution of the Pt catalyst at high potentials. They were becoming greater with increasing potentials. Furthermore, it is noticeable that cyclic potential scan must be conducted in order to ensure that the oxidized Pt could be completely reduced.

3.2.2. The influence of the initial potentials in CV

In order to investigate the influence of the starting potentials on the oxidation of the adsorbed sulfur species, potential scans beginning from various potentials were performed. Each single cell was poisoned by 100 ppm SO_2 for 10 min at 0.65 V, with the cell temperatures and humidification temperature all fixed at 70 °C. The potential scans were performed after keeping the initial potentials for 60 s. All the conditions were the same as that in the CV scans (Section 2). In each scan, the potential swept positively to 1.4 V, ensuring all the possible oxidation of adsorbed sulfur. Then it swept negatively to 0.3 V, completing the process for Pt oxide reduction. All the scans are plotted in Fig. 10.

As shown in Fig. 10, the O-oxidation peak areas increase with the ascending initial potentials. It implies that there were more charges from the sulfur oxidation. The phenomenon may be resulted from the existing of different chemical valences of the adsorbed sulfur species on the Pt surface. The reasons will be discussed in detail in Section 3.3.1.

3.3. Potential dependence of sulfur poisoning

3.3.1. Valences of adsorbed sulfur

Assuming that the same amount of adsorbed sulfur is oxidized to sulfate in each scan, and the adsorbed sulfur with zero valence at

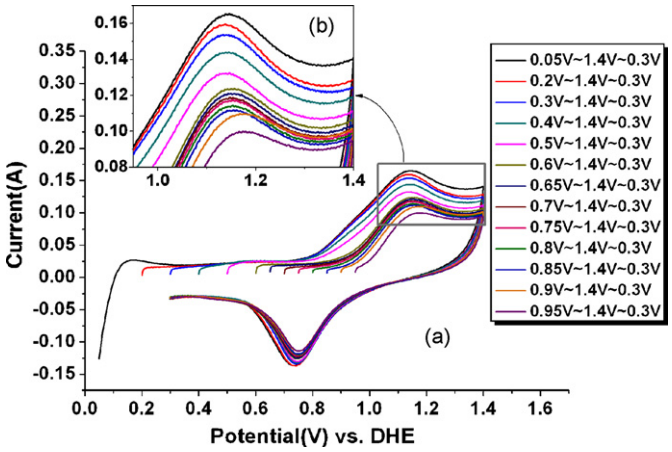

Fig. 10. (a) Potential scans starting from different potentials after the cathode being exposed to 100 ppm SO_2 for 10 min at 0.65 V. (b) Enlarged part of O-oxidation peaks in cyclic voltammetry spectra. T_{cell} = 70 °C, humidification temperatures of the anode and the cathode: 70 °C.

0.05 V is oxidized when the potential was sweeping to 1.4 V, accompanying with a 6-electron transfer per sulfur atom. So, by using Eq. (5), charges sulfur oxidation in each scan (Fig. 10) could be obtained. By comparing them with that in the cycle starting from 0.05 V, the numbers of transferred electrons per sulfur atom during the cathode potential scans from a given value to 1.4 V could be obtained. All the calculated results are exhibited in Fig. 11.

It is indicated in Fig. 11 that when the initial potential was between 0.05 and 0.65 V, the existing chemical valences of the adsorbed sulfur species were from 0 to 4. It implied that the adsorbed SO_2 had been reduced in this potential range. When the initial potential was 0.65 V, about 2 electrons per sulfur atom was transferred during the oxidation of the adsorbed sulfur up to 1.4 V. The result implies that almost no charges had been transferred when SO_2 was adsorbed on the Pt surface at 0.65 V, and SO_2 was keeping a valence state of 4 after adsorption. When the initial potential was in the range of 0.65–0.9 V, less than 2 electrons per sulfur atom was transferred. It is evident that some adsorbed sulfur had been oxidized. Obviously, the result is inconsistent with the fact that the adsorbed sulfur could only be oxidized at potentials over 0.9 V. The explanation will be given in Section 3.3.2.

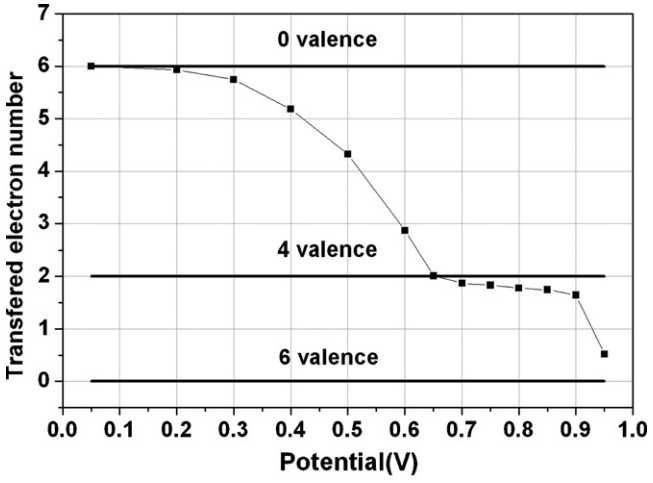

Fig. 11. Number of charge transfer from various potentials to 1.4 V.

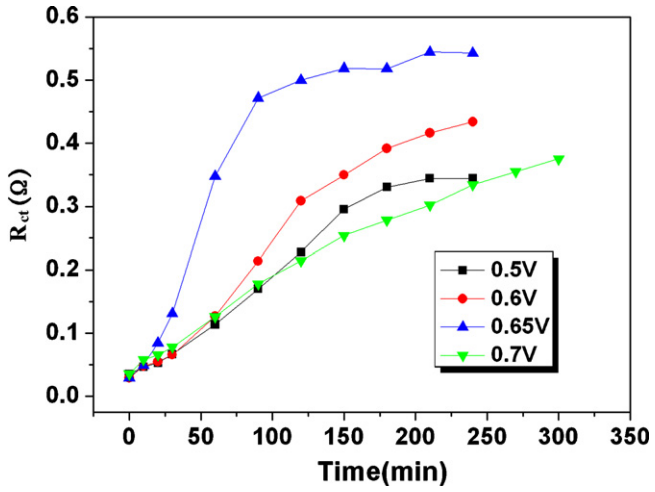

Fig. 12. Change of R_{ct} calculated from EC at 0.5 V, 0.6 V, 0.65 V and 0.7 V during the cathode exposure to 25 ppm SO_2. T_{cell} = 70 °C, humidification temperatures of the anode and the cathode: 70 °C.

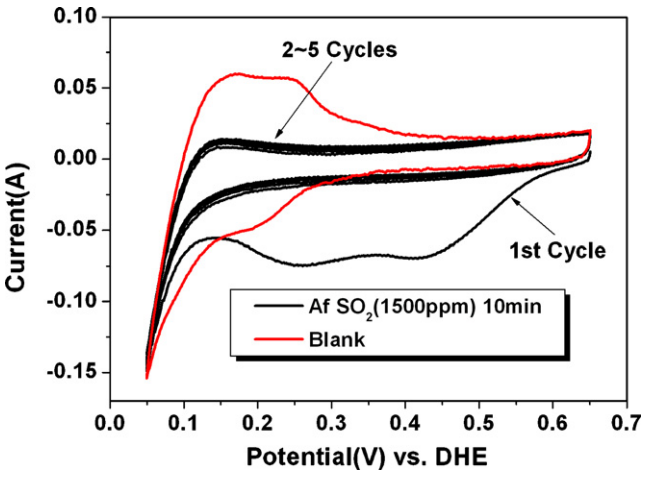

Fig. 13. Cyclic voltammetry spectra after the cathode being exposed to 1500 ppm SO_2 for 10 min (0.65 V~0.05 V~0.65 V). T_{cell} = 70 °C, humidification temperatures of the anode and the cathode: 70 °C.

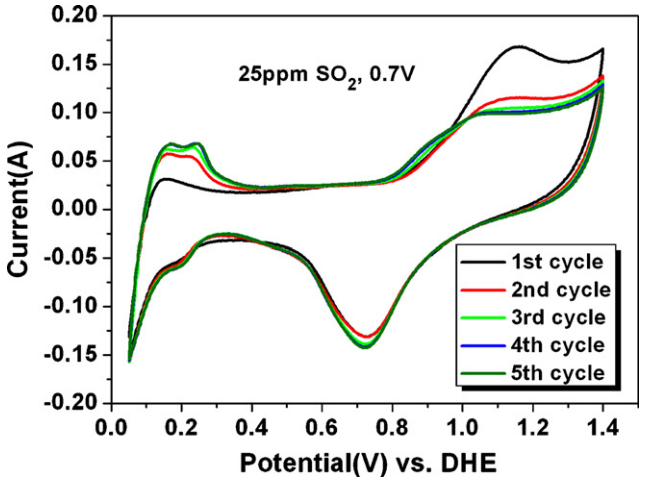

Fig. 14. CV spectra of first 5 cycles after the cathode being poisoned by 25 ppm SO_2 for 5 h at 0.7 V. T_{cell} = 70 °C, humidification temperatures of the anode and the cathode: 70 °C.

Furthermore, only about 0.5 electron per sulfur atom transfer occurred at 0.95 V, revealing that most of the SO_2 adsorbed on the Pt surface had been oxidized.

3.3.2. *Effects of potential on SO_2 poisoning in PEMFC*

As has been mentioned above, the SO_2 adsorbed on the Pt surface is not always in a molecular state, and it can be oxidized or reduced at different potentials. Thus, the PEMFCs would show distinct performances under different voltages.

All the cells were poisoned by 25 ppm SO_2 in air at 0.5, 0.6, 0.65 and 0.7 V, respectively. The cell temperature and the humidification temperature were both 70 °C. EIS was measured in different poisoning periods at each voltage. Changes in R_{ct} which was calculated from EC at each voltage were plotted in Fig. 12. As can be seen in Fig. 12, R_{ct} grew most rapidly when the cell was poisoned at 0.65 V. So it can be deduced that SO_2 adsorption would impact on the performances of the PEMFCs most severely at 0.65 V.

However, as we know, reduction could not desorb sulfur dioxide from the Pt surface. So the advantage of lower voltages during the poisoning process should be investigated further. To analyze the changes during the reduction of the adsorbed sulfur on the Pt surface, novel CV scans were applied. Each cycle began at 0.65 V, then down to 0.05 V, and back to 0.65 V again. Fig. 13 shows the CV spectra after a cathode exposure to 1500 ppm SO_2 for 10 min. Two evident peaks can be found at 0.26 and 0.45 V in the first cycle. The ECA changed from 19.71 $cm^2\ mg^{-1}$ in the first cycle to 21.57 $cm^2\ mg^{-1}$ in the fifth cycle.

It has been reported that some adsorbed sulfur was lying on the Pt surface with a bridge geometry, such that each sulfur dioxide occupied two Pt sites through the S and O atoms [19]. The two reduction peaks may be corresponding to Eqs. (8) and (9)

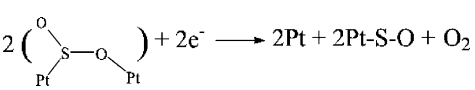

(8)

$$2Pt\text{–}S\text{–}O + 2e^- \rightarrow 2Pt\text{–}S + O_2 \quad (9)$$

After reduction down to 0.05 V, the Pt sites bound to O were released. It means that the adsorbed sulfur dioxide bound to the Pt surface became less stable and tended to be oxidized easily. Due to the increased number of sites, ECA had grown accordingly. This can be used to explain well that when the cell voltage was below 0.65 V, lower voltage was advantageous during the SO_2 poisoning of the PEMFCs.

Quijada et al. [15] have considered that adsorbed sulfur could be oxidized over 0.65 V, but adsorbed SO_2 would inhibit strongly the further oxidation of the sulfur species. Fig. 14 shows the first 5 cycles of the CV spectra after the cathode was poisoned at 0.7 V by 25 ppm SO_2 for 5 h. As can be seen in the figure, the starting potentials of sulfur oxidation decreased because of the loss of sulfur coverage. So it can be deduced that when the cell was operating at 0.7 V, some of the adsorbed SO_2 could be oxidized before the consequent adsorption. So the durability was better than that at 0.65 V. It was also consistent with the previous result that less than 2 electrons had been transferred from 0.7 to 1.4 V. But after the cathode was exposed to 25 ppm SO_2 for 5 h at 0.7 V, most of the Pt sites had been covered by SO_2. Because of the high lateral dipole interactions between the neighbouring adsorbed SO_2, further oxidation was strongly inhibited till the voltage had risen up to over 0.9 V.

4. Conclusions

The behavior of the poisoning of the PEMFC cathode by SO_2 was studied. When a PEMFC cathode was exposed to SO_2, some of the surface active sites of the Pt catalyst were covered by adsorbed

sulfur species. The charge transfer resistance increased due to the loss of ECA, and the PEMFC performance declined accordingly.

Both SO_2 adsorption and oxidation on Pt showed high potential dependence. The initial potential of sulfur oxidation was between 0.9 and 0.95 V. And only CV, whose upper limit could reach to over 1.05 V, could be used to recover completely the poisoned cathode. Reduction down to 0.05 V could cause an increase in ECA. It attributed to the breaking of the bridge geometry in which some undissociated SO_2 molecules were bonded to two sites through S and O. After that, some Pt sites originally bonded to O became active. SO_2 molecules could be adsorbed on Pt surface without charge transfer at 0.65 V and could be reduced below 0.65 V. So when the PEMFC was operating at a constant voltage lower than 0.65 V, better durability could be observed because of a higher availability of the catalyst sites.

Acknowledgements

This work was financially supported by the National High Technology Research and Development Program of China (863 Program, No. 2007AA11A106) and the National Natural Science Foundation of China (No. 20636060).

We also appreciate Prof. Dongbai Liang very much who provided a very professional English writing help and offered a polished revision.

References

[1] S. Knights, N. Jia, C. Clug, J. Zhang, Fuel Cell Seminar (2005).
[2] E. Brosha, F. Garzon, B. Pivovar, T. Rockward, J. Valeria, F. Uribe, 2005 Mid Year DOE Fuel Cell Program Review.
[3] Y. Garsany, O.A. Baturina, K.E. Swider-Lyons, 212th Meeting of the Electrochemical Society, 2007.
[4] Y. Nagahara, S. Sugawara, K. Shinohara, J. Power Sources 182 (2008) 422–428.
[5] F. Jing, M. Hou, W. Shi, J. Fu, H. Yu, P. Ming, B. Yi, J. Power Sources 166 (2007) 172–176.
[6] R. Motadi, W.-K. Lee, J.W. Van Zee, J. Power Sources 138 (2004) 216–225.
[7] F. Uribe, W. Smith, M. Wilson, FY 2003 Progress Report, LANL.
[8] R. Borup, E. Brosha, F. Garzon, DOE Hydrogen, Fuel Cells and Infrastructure Technologies, 2007 Kickoff Meeting.
[9] Y. Garsany, O.A. Baturina, K.E. Swider-Lyons, J. Electrochem. Soc. 154 (2007) B670–B675.
[10] T. Loučka, J. Electroanal. Chem. 31 (1971) 319–332.
[11] A.Q. Contractor, H. Lal, J. Electroanal. Chem. 93 (1978) 99–107.
[12] E.S. Matveeva, V.A. Shepelin, E.V. Kasathin, Sov. Electrochem. 18 (1982) 634–640.
[13] A.Q. Contractor, H. Lal, J. Electroanal. Chem. 103 (1979) 103–117.
[14] C. Quijada, J.L. Vázquez, J.M. Pérez, A. Aldaz, J. Electroanal. Chem. 372 (1994) 243–250.
[15] C. Quijada, A. Rodes, J.L. Vázquez, J.M. Pérez, A. Aldaz, J. Electroanal. Chem. 374 (1995) 217–227.
[16] C. Quijada, A. Rodes, J.L. Vázquez, J.M. Pérez, A. Aldaz, J. Electroanal. Chem. 378 (1995) 105–115.
[17] I.R. Moraes, M. Weber, F.C. Nartt, Electrochim. Acta 42 (4) (1997) 617–625.
[18] N. Wagner, J Appl. Electrochem. 32 (8) (2002) 859–863.
[19] C. Quijada, A. Rodes, F. Huerta, J.L.J.L. Vázquez, Electrochim. Acta 44 (1998) 1091–1096.